Probing the Nature of the Co^{III} Ion in Cobalamins − Spectroscopic and Structural Investigations of the Reactions of Aquacobalamin (Vitamin B_{12a}) with Ambident Nucleophiles

Christopher B. Perry,[a] Manuel A. Fernandes,[a] Kenneth L. Brown ,[b] Xiang Zou,[b] Edward J. Valente,[c] and Helder M. Marques*[a]

Keywords: Cobalamins / Ambidentate ligands / Cobalt / Bioinorganic chemistry / X-ray diffraction

The rate of substitution of the H_2O β-ligand in aquacobalamin (vitamin B_{12a}) is surprisingly fast for Co^{III}. This may arise as a result of transfer of electron density to Co^{III} by the corrin, conferring on the metal atom a softer and more labile character, and would require electronic communication between the equatorial ligand and the axial coordination sites of the metal atom. We have substituted H_2O in B_{12a} with the ambidentate nucleophiles SCN^-, $SeCN^-$, NO_2^- and $S_2O_3^{2-}$, examined the UV/Vis spectra of the resultant complexes, crystallised them, and determined their structures by X-ray diffraction methods. The UV/Vis spectra of these complexes, as well as those of H_2OCbl^+, SO_3Cbl^- and MeCbl, were fitted by Gaussian functions. The principal bands move to lower energy in response to an increase in donation of electron density from the axial ligand, demonstrating direct electronic communication between the axial and the equatorial ligands. In the solid state, the thiocyanato ligand in SCNCbl is coordinated through N, although ^{13}C NMR spectroscopy shows that the complex exists as a mixture of two linkage isomers in solution. $SeCN^-$, NO_2^- and $S_2O_3^{2-}$ are coordinated through the softer available donor in each case (Se, N and S, respectively). There is a regular ground-state *trans* effect such that as the donor power of the β-ligand increases, the *trans* $Co–N_{ax}$ bond length increases. A survey of the structures available in the CSD shows that this preference for the softer donor atom in ambidentate nucleophiles is not unusual in Co^{III} complexes. The Co–N bond length in SCNCbl is marginally long for coordination to Co^{III}, but the axial bond lengths of the other complexes are as expected. Hence, whereas the corrin macrocycle clearly imparts lability on Co^{III}, presumably by transfer of electron density onto the metal atom, this is insufficient to have a major effect on the ground-state structures of its complexes.

Introduction

We have previously[1] studied the kinetics of the ligand substitution reactions of coordinated H_2O in aquacobalamin (H_2OCbl^+, vitamin B_{12a}, Figure 1) by a series of small anionic ligands ($S_2O_3^{2-}$, SCN^-, NO_2^-, NCO^-, $SeCN^-$, N_3^-) and determined the second-order rate constants, k_{II}, corresponding to the bimolecular reaction of Equation (1), where bzm is the base 5,6-dimethylbenzimidazole that occupies the lower (α) coordination site of aquacobalamin, N_4 represents the equatorial corrin ligand, and charges are omitted for convenience. We calculated the activation parameters $\Delta H^{\ddagger}$ and $\Delta S^{\ddagger}$ from the temperature dependence of k_{II} and the Mulliken charge population of the donor atoms from semiempirical molecular orbital calculations using the PM3 model.[2,3]

$$\text{bzm-Co(N}_4\text{)-OH}_2 + \text{L} \xrightarrow{k_{II}} \text{bzm-Co(N}_4\text{)-L} + \text{H}_2\text{O} \quad (1)$$

If we assumed, irrespective of the thermodynamically preferred product, that (i) SCN^- reacts through N, (ii) NO_2^- reacts through N, (iii) NCO^- reacts through O, (iv) $S_2O_3^{2-}$ reacts through S and (v) $SeCN^-$ reacts through Se in the microscopic process that determines the magnitude of the activation parameters, then a three-dimensional plot of $\Delta H^{\ddagger}$ as a function of the energy, E_σ, of the frontier orbital with σ symmetry on the donor atom, and the Mulliken population (MP) of that atom, yielded a planar surface ($r^2 = 0.81$; $f = 6.30$; 92% confidence that the correlation is not due to random chance) that showed that $\Delta H^{\ddagger}$ decreases, and the reactions speed up, as the MP and E_σ decreased. A similar correlation with $\Delta S^{\ddagger}$ was observed ($r^2 = 0.95$; $f =$

[a] Molecular Sciences Institute, School of Chemistry, University of the Witwatersrand,
P. O. Wits, Johannesburg 2050, South Africa
Fax: (internat.) + 27-11/717-6749
E-mail: hmarques@aurum.chem.wits.ac.za
[b] Department of Chemistry and Biochemistry, Ohio University, Athens, OH 75701, United States of America
[c] Department of Chemistry, Mississippi College, Clinton, MS 39058, United States of America
Supporting information for this article is available on the WWW under http://www.eurjic.org or from the author.

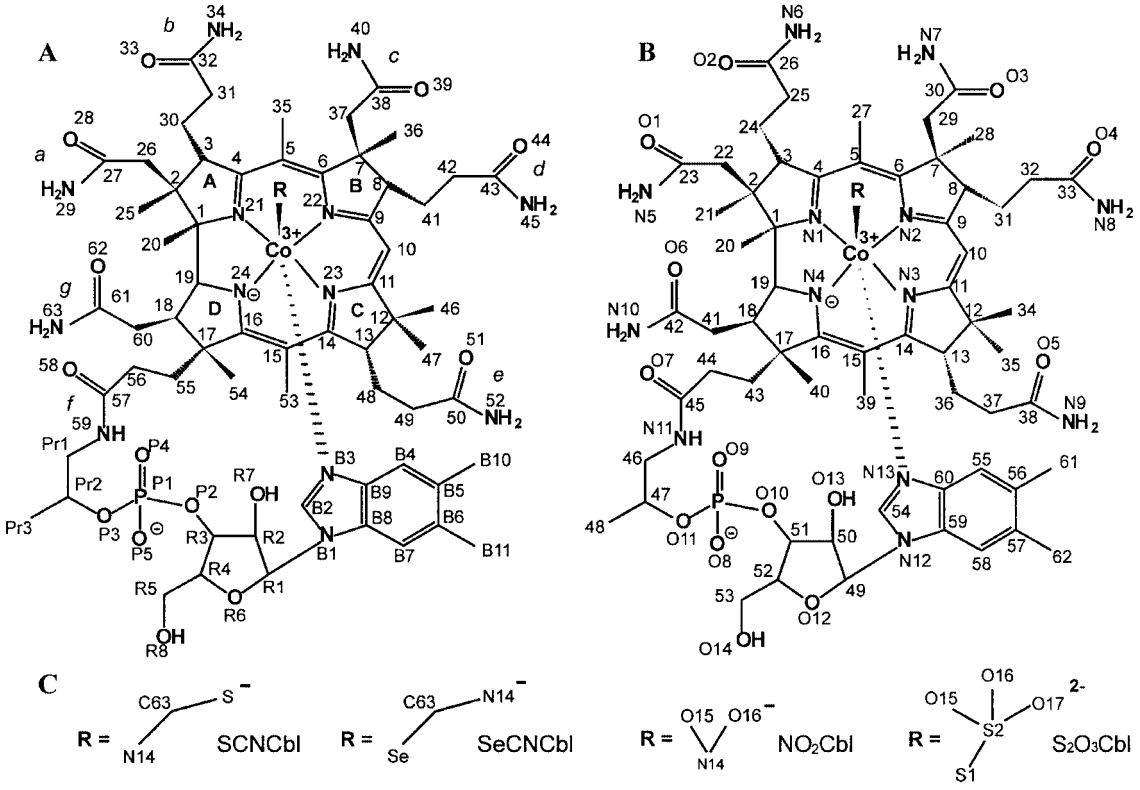

Figure 1. (A) The common numbering scheme and standard view of the cobalt corrinoids; aquacobalamin (vitamin B_{12a}) has a Co^{III} ion coordinated in the equatorial plane by the macrocyclic ligand corrin; the equatorial ligand on the lower (α) face is 5,6-dimethylbenzimidazole (bzm), whilst that on the upper (β) face is R = H_2O; coordinated H_2O is readily replaced by ligands from solution in reactions that are surprisingly fast for Co^{III}; in this view, the C13···C17 portion of the molecule is known as the southern quadrant, C7···C13 as the eastern quadrant, and so on; (B) and (C) show the crystallographic numbering scheme used in this work

26.6; > 99% confidence that the correlation is not due to random chance), with $\Delta S^{\ddagger}$ decreasing and the reaction becoming slower with decreasing MP and E_{σ}. There is therefore a compensating effect between $\Delta H^{\ddagger}$ and $\Delta S^{\ddagger}$, the origin of which, related to the density of states in the transition state, was discussed.

Co^{III} usually behaves as a hard (class a) metal ion.[4] The curious mixture of the kinetically favoured donor atom in the reactions of B_{12a} with ambident nucleophiles (the harder of the two donors is preferred in the reaction with SCN^- and NCO^-, but the softer donor in the case of $S_2O_3^{2-}$, NO_2^- and $SeCN^-$), may be evidence of a somewhat softer metal ion character due to a transfer of electron density from the corrin ring. It has previously been pointed out[5,6] that the rates of ligand substitution reactions at the Co^{III} centre in the cobalamins are surprisingly fast for Co^{III}, which is a classic example of an inert transition metal ion. Thus, the lability ratio of the metal ion towards substitution in corrin, porphyrin, cobaloxime and macrocyclic saturated ammine systems is 10^9:10^6:10^4:1 (Figure 2). We suggest that this considerable *cis*-labilising effect of the corrin is due to the transfer of electron density from the macrocycle to the metal ion, conferring on the metal atom some element of labile character characteristic of Co^{II}. For this

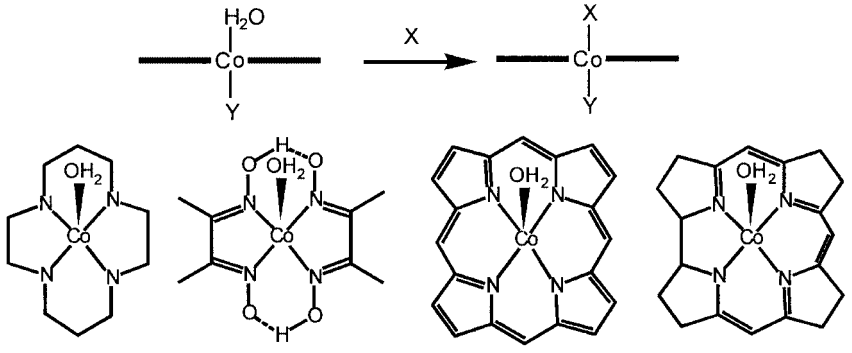

Figure 2. Changing the equatorial ligand system from (left to right) ammine to cobaloxime to porphyrin and corrin causes the rate of substitution of the axial H_2O to increase approximately in the ratio 1:10^4:10^6:10^9 [5]

to be a feasible explanation for the kinetic behaviour, direct electronic communication between the corrin ring and the axial coordination site of Co^{III} is required. To this end, we have shown[5] that substitution of the H centre at the C10 position with Cl (Figure 1), and an increase in the donor power of the axial ligand ($H_2O < CN^- < Me$) increased the C10−Cl bond length as well. Moreover, Mulliken charges obtained from semiempirical MO calculations using the ZINDO/1 model[7,8] (which correlate well with ^{13}C NMR chemical shifts and which may therefore be used to determine the pattern of electron distribution in these complexes) confirmed that the charge density on the metal ion, on the N donor atoms of the corrin, and on the corrin C atoms is affected by the donor power of the axial ligand. We have also shown recently[9] that if the H atom at C10 is replaced by an electron-withdrawing NO group, the metal ion is deactivated towards ligand substitution, i.e., 10-NO-H_2OCbl^+ is inert towards substitution of the axial H_2O molecule by pyridine and N_3^-, and reacts only slowly with CN^-.[10] The conferring of some labile character on the metal atom may be an important aspect of the biological chemistry of coenzyme B_{12} (AdoCbl, adenosylcobalamin; R = 5′-deoxyadenosyl in Figure 1,) since the first step in AdoCbl-catalysed enzymatic reactions is homolysis of the Co−C bond to produce Co^{II} and an alkyl radical,[11−13] a process that is catalysed by a factor of 10^{12} or higher.[14−16] There is a clear mechanistic advantage from increasing the electron density on the metal atom and increasing its lability. It has been shown, for example, that reduction of methylcobalamin to Co^{II} results in a $> 10^{15}$ rate enhancement of thermal homolysis of the Co−C bond[17] and Co^{II} corrinoids are either five-coordinate[18,19] or, at most, the β-ligand interacts very weakly with the metal centre.[18] It is an attractive hypothesis that the corrin transfers significant electron density onto Co^{III}, in effect conferring some labile Co^{II}-like character to it, and that the protein, on binding the coenzyme B_{12} cofactor and perhaps the substrate, modulates this effect further thereby activating the Co−C bond towards homolysis.

The axial Co−N bonds to the bzm base tend to be long (2.26−1.95 Å),[20] whereas the Co−N bond lengths in the equatorial plane of Co^{III} are similar to those in Co^{III}−ammine complexes (1.96−1.99 Å), as Lenhert pointed out.[21] This may be merely a consequence of the steric demands of bzm (and, in particular, the clashing of the B4 proton with the corrin ring), rather than a structural response to low-spin Co^{II}-like character of the metal atom. In this regard it is probably significant that the Co−N(imidazole) bond in Co-β-cyanoimidazolylcobamide, where the bzm base has been replaced by a sterically much less demanding imidazole,[22] is "normal", with a distance of 1.97 Å. In methionine synthase[23] and in methylmalonyl CoA mutase[24] the bzm base is replaced by an imidazole residue from the protein. The $Co-N_{ax}$ bond length in the former is not unusual (2.2 ± 0.2 Å), although the resolution is relatively low. In the latter, the B_{12} cofactor is present as Co^{II}, and there is a long $Co-N_{ax}$ bond (2.5 ± 0.1 Å), despite attempts to constrain this bond length to more normal values during the refinement process.[25] There is no crystal structure of imidazolylcob(II)amide, but a comparison of the $Co-N_{ax}$ bond lengths of cyanocobalamin and cyanoimidazolylcobamide strongly suggests[26] that the $Co-N_{ax}$ bond length is as much as 0.4 Å longer when the cofactor is bound to the protein.

The very rich chemistry of organocobalamins is further evidence that the Co^{III} ion in the cobalamins behaves very differently from a classical, hard and inert d^6 ion. As mentioned, the first step in the AdoCbl-catalysed enzymatic reactions is formation of Co^{II} and a radical (i.e., the Co−C bond could be formulated as $Co^{II} + R^{\cdot}$). Both UV/Vis and resonance Raman spectroscopic results suggest that an alkylcobalamin is best viewed as a compound intermediate between Co^{III} and a carbanion.[27] The transfer of a methyl group from methylcobalamin to homocysteine produces Co^{I}, which then acts as a powerful nucleophile towards the methyl group donor, N5-methyltetrahydrofolate,[28] i.e. the Co−C bond could be formulated as $Co^{I} + R^{+}$.

In this paper we investigate the *cis* influence (to demonstrate the electronic communication between the axial coordination site and the corrin ring) and *trans* influences (to extend further the well-established *trans* influence in the cobalamins to the compounds under investigation) and then explore further the nature of the Co^{III} ion by addressing two questions. Firstly, when offered an ambident nucleophile with two donor atoms of different hardness, what is the thermodynamically favoured product? Secondly, is there any evidence in the solid state for an elongation of the axial bond to such a nucleophile? To this end, we have displaced H_2O in B_{12a} with $S_2O_3^{2-}$, SCN^-, NO_2^-, and $SeCN^-$ and crystallised the resultant compounds in order to determine their structures by X-ray diffraction analysis. We have been unable to crystallise CNOCbl, which slowly decomposes to CNCbl. Pertinent to this work is a report by Randaccio[29] and co-workers on the crystal structures of sulfitocobalamin, SO_3Cbl^-. This was found to be *S*-bound with a Co−S bond length of 2.134(7) Å. We are currently using NMR-restrained molecular modelling techniques to examine the structures of these compounds in solution and will report on those results elsewhere.

Results

UV/Vis Spectra

The UV/Vis spectra of H_2OCbl^+, NO_2Cbl, SCNCbl, $S_2O_3Cbl^-$, SeCNCbl, SO_3Cbl^- and MeCbl are shown in Figure 3. The spectrum of, for example, H_2OCbl^+ with its well-defined γ-band (the prominent band around 350 nm), has been referred to as a "typical" cobalamin spectrum, whereas that of MeCbl (for example), where the γ-band is apparently less well defined, and a greater number of bands are discernible especially in the shorter wavelength region, has been termed an "atypical" spectrum.[30] On this basis, one would classify the spectra of H_2OCbl^+, NO_2Cbl and SCNCbl as "typical" and those of $S_2O_3Cbl^-$, SeCNCbl, SO_3Cbl^- and MeCbl as "atypical".

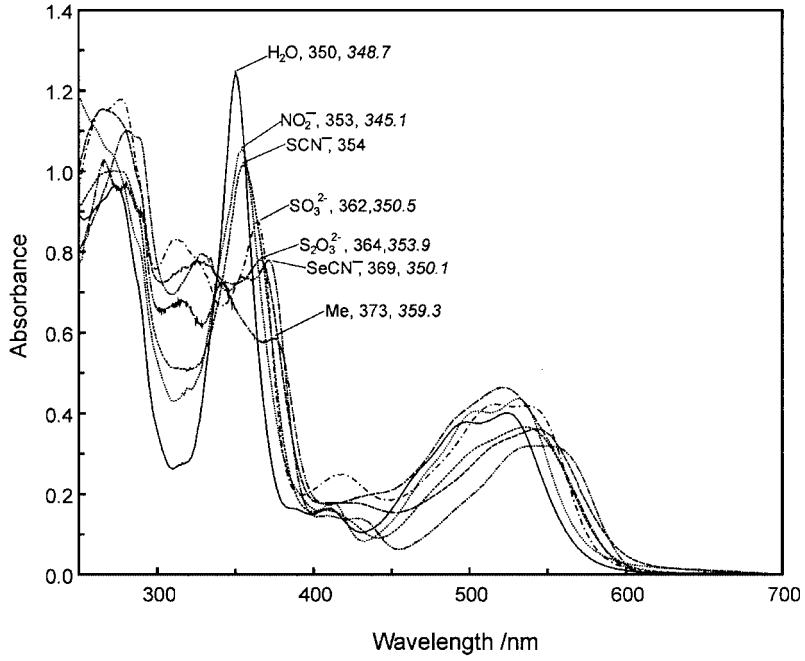

Figure 3. The UV/Vis spectra of cobalamin complexes; the identity of the β-axial ligand is given in each case, as is the observed position [nm] of the maximum absorption in the γ-band region of the spectrum; the γ-band envelope consists of three overlapping transitions, as shown by a Gaussian analysis of the spectra (see text, and Figure 4); the mean position of these three transitions is given in italics

An example of the fitting of the spectra under discussion with a series of Gaussian functions is shown in Figure 4. Either 11 (H_2OCbl^+, NO_2Cbl), 12 ($S_2O_3Cbl^-$, SeCNCbl, SO_3Cbl^-) or 13 (MeCbl) Gaussian functions were required to adequately fit the spectra. The results are listed in Table S1 of the Supporting Information. The γ-band of the corrins is best modelled as the overlap of three transitions, as are the αβ-bands (in the 450−600 nm region). In the case of NO_2Cbl, two of the components of the γ-band region overlap closely, and the region can only be resolved into two component Gaussian functions.

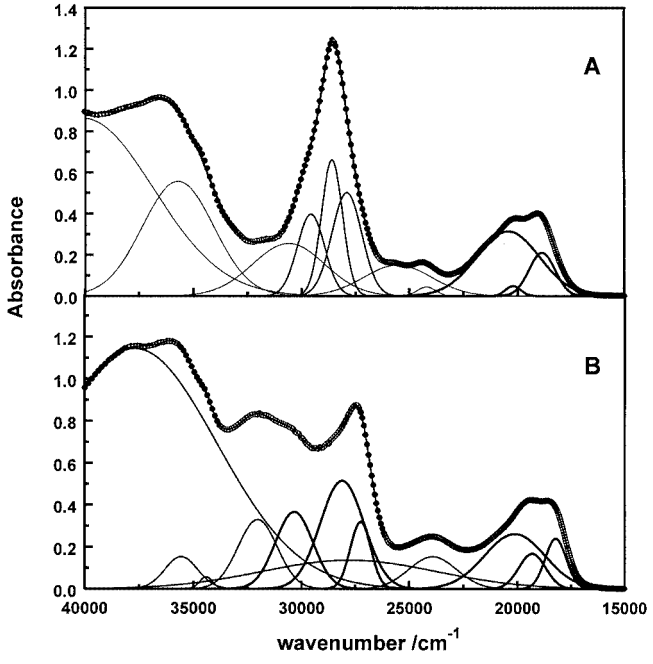

Figure 4. Resolved UV/Vis spectra of (A) H_2OCbl^+ and (B) SeCNCbl; The γ-band in each case is best fitted by three Gaussian functions (shown as bold lines); the circles are the experimental data and the line through the circles is the sum of the individual Gaussian bands

Structure of SCNCbl

SCNCbl crystallises in the orthorhombic space group $P2_12_12_1$ (R_1 = 8.75%, Figure 5). The experimental data are summarised in Table 1. The thiocyanato ligand is coordinated through N [Co−N = 1.954(11) Å] in a bent fashion [Co−N−C = 146.2(11)°], and positioned over C15 (Figure 6). Some of the bond lengths and bond angles involving the metal ion are summarised in Table 2.

As is usually found in the crystal structures of cobalt corrinoids, several solvent water molecules are incorporated, and they are extensively hydrogen-bonded to the amide side chains of the corrin. Possible hydrogen bonds were identified by standard methods.[31] An amide proton of N40 in the *c* side chain appears to be hydrogen-bonded to the N atom of coordinated SCN^- (N40···NCS = 3.309Å, N40−H−NCS = 161°). N52 of the *e* side chain amide group is hydrogen-bonded to N45 of the *d* side chain of a neighbouring molecule, whilst O51 acts as a hydrogen bond acceptor to N63 of the *g* side chain. The second N63 proton is hydrogen-bonded to O33 of the *b* side chain of a neighbouring molecule. Both hydroxy groups of the ribose act as hydrogen bond donors towards solvent water molecules.

Structure of SeCNCbl

SeCNCbl crystallises in the orthorhombic space group $P2_12_12_1$ (R_1 = 7.46%, Figure 5). The experimental data are

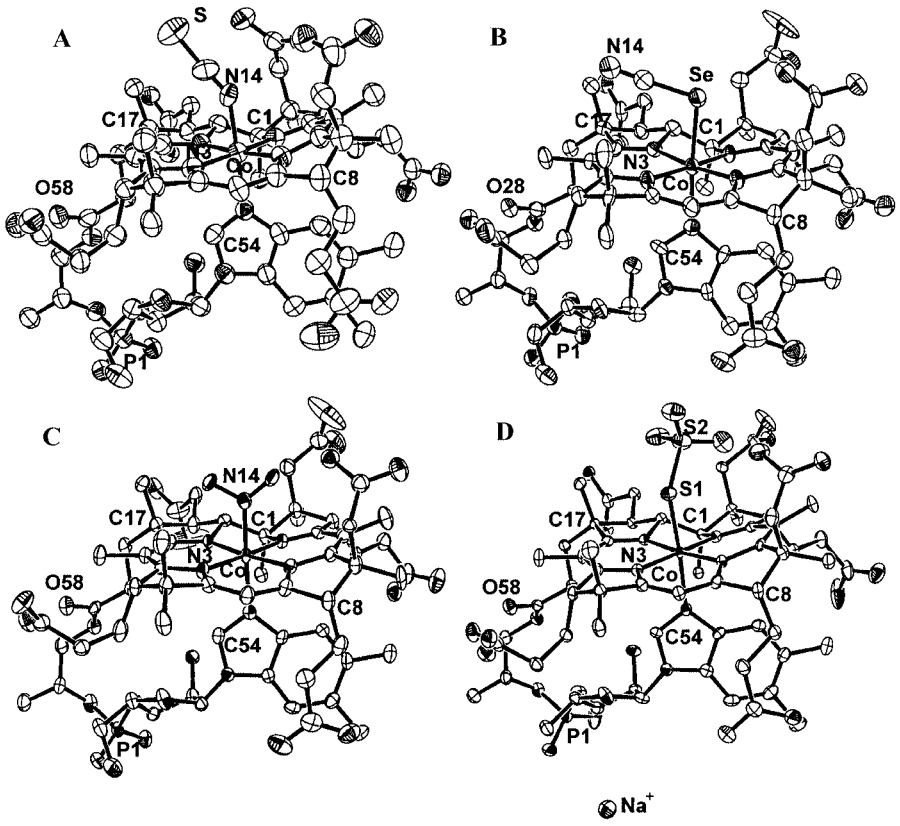

Figure 5. ORTEP diagram of (A) SCNCbl (25% probability contours), (B) SeCNCbl (50% probability contours), (C) NO_2Cbl (50% probability contours, with disorder in the orientations of the NO_2 ligand, and the *c* and *e* side chains removed for clarity), (D) $Na^+S_2O_3Cbl^-$ (50% probability contours)

summarised in Table 1. The selenocyanato ligand is coordinated through Se [Co−Se = 2.394(2) Å] in a bent fashion [Co−Se−C = 104.3(3)°] and the ligand is orientated over the southern quadrant of the molecule (Figure 6). Some of the bond lengths and bond angles involving the metal ion are summarised in Table 2. We were also able to grow crystals rapidly by using a near-saturated solution of B_{12a} in the presence of 0.05 mol·dm^{-3} KSeCN (crystals were obtained in a few hours). Although the crystal quality was poor, the diffraction data (not shown) were good enough for refinement to a level that showed unambiguously an *Se*-bound selenocyanato ligand.

The amide NH groups of the *a*, *b*, *c*, *d*, *e* and *f* side chains act as hydrogen bond donors towards solvent water molecules, whilst the *d* and *e* amide groups are also hydrogen-bonded to the carbonyl group of the *a* side chains of neighbouring molecules. The *g* side chain is hydrogen-bonded to the *b* and *e* side chains of neighbouring molecules. The R7 and R8 hydroxy groups [see Figure 1(A)] are hydrogen-bonded to solvent water molecules.

Structure of NO_2Cbl

NO_2Cbl crystallises in the orthorhombic space group $P2_12_12_1$ (R_1 = 7.16%, Figure 5). The experimental data are summarised in Table 1. The nitro ligand is coordinated through N [Co−N = 1.941(5) Å] and the ligand is disordered over two positions (Figure 6). In the first position [0.82(10) occupancy], the two oxygen atoms point towards C10 and the C1−C19 bond [N−O−N = 121.6(5)°]. In the second position [0.18(10) occupancy] they are virtually orthogonal to this, pointing towards C5 and C15 [N−O−N = 111.2(15)°]. Some of the bond lengths and bond angles involving the metal ion are summarised in Table 2.

As with the other structures, there is extensive hydrogen bonding of the amide side chains. One of the *c* side chain amide protons is hydrogen-bonded to the N atom of the coordinated NO_2 ligand. Hydrogen bonding occurs between the amide protons of the *e*, *d* and *g* side chains of one molecule, and the *a* side chain of one neighbouring molecule and the *a* and *b* side chains of a second neighbouring molecule, respectively. The amide proton of the *a* side chain is hydrogen-bonded to the O atom of the acetone solvent molecule in the same unit cell, whilst one of the *d* side chain amide protons is hydrogen-bonded to a neighbouring acetone molecule. The amide groups of the *b*, *c*, *e*, *f* and *g* side chains are hydrogen-bonded to water molecules.

Structure of $S_2O_3Cbl^-$

$Na^+S_2O_3Cbl^-$ crystallises in the orthorhombic space group $P2_12_12_1$ (R_1 = 5.88%, Figure 5). The experimental data are summarised in Table 1. The thiosulfate ligand is coordinated through S [Co−S = 2.2861(11) Å]. The ligand points towards C1 and comes within van der Waals contact with the *a* side chain (Figure 6); as a consequence, the li-

Table 1. Experimental data for the crystal structure determination of XCbl; X = SCN^-, $SeCN^-$, NO_2^-, $S_2O_3^{2-}$ (* excludes solvate molecules)

	SCNCbl	SeCNCbl	$S_2O_3Cbl^-$	NO_2Cbl
CCDC-	-185962	-185963	-185964	-185965
Empirical formula*	$C_{63}H_{88}CoN_{14}O_{14}PS$	$C_{63}H_{88}CoN_{14}O_{14}PSe$	$C_{62}H_{88}CoN_{13}NaO_{32}PS_2$	$C_{62}H_{88}CoN_{14}O_{16}P$
Molecular mass	1387.4	1434.3	1375.4	1432.4
Temperature [K]	173(2)	123(2)	123(2)	123(2)
Wavelength [Å]	0.71073	0.71073	0.71073	0.71073
Crystal system	orthorhombic	orthorhombic	orthorhombic	orthorhombic
Space group	$P2_12_12_1$	$P2_12_12_1$	$P2_12_12_1$	$P2_12_12_1$
Unit cell dimensions [Å]	a = 16.353(4) b = 20.823(5) c = 23.933(6)	a = 15.955(6) b = 21.338(7) c = 23.646(8)	a = 16.020(3) b = 20.922(3) c = 24.722(4)	a = 16.120(4) b = 20.974(6) c = 23.309(6)
Volume [$Å^3$]	8150(3)	8050(5)	8286(2)	7881(4)
Z	4	4	4	4
Density (calcd.) [gcm^{-3}]	1.352	1.406	1.437	1.394
Absorption coefficient [mm^{-1}]	0.342	0.772	0.374	0.328
F(000)	3540	3608	3816	3530
Crystal size [mm]	0.36 × 0.20 × 0.20	0.34 × 0.17 × 0.16	0.44 × 0.34 × 0.30	0.40 × 0.22 × 0.22
θ range for data collection [°]	1.30−23.25	1.29−24.99	1.51−28.01	1.31−25.50
Index ranges	$-17 \le h \le 17$ $-22 \le k \le 22$ $-5 \le l \le 26$	$-18 \le h \le 18$ $-25 \le k \le 23$ $-28 \le l \le 22$	$-20 \le h \le 10$ $-26 \le k \le 27$ $-29 \le l \le 30$	$-19 \le h \le 18$ $-15 \le k \le 25$ $-28 \le l \le 25$
Reflections collected	27133	35010	48888	38172
Independent reflections	10141 [R(int) = 0.0804]	13094 [R(int) = 0.0826]	17883 [R(int) = 0.0275]	14186 [R(int) = 0.0380]
Completeness to θ	23.25°, 90.3%	24.99°, 95.5%	28.01°, 91.8%	25.50°, 98.5%
Absorption correction	semiempirical from equivalents	semiempirical from equivalents	semiempirical from equivalents	semiempirical from equivalents
Max./min. transmission	0.9347/0.8867	0.8864/0.7792	0.8960/0.8527	0.9313/0.8799
Refinement method	full-matrix least squares on F^2	full-matrix least squares on F^2	full-matrix least squares on F^2	full-matrix least squares on F^2
Data/restraints/parameters	10141/1/1001	13094/7/988	17883/39/1063	14186/81/1043
Goodness-of-fit on F^2	1.047	1.049	1.085	1.069
Final R indices [$I > 2\sigma(I)$]	R_1 = 0.0875, wR_2 = 0.2041	R_1 = 0.0746, wR_2 = 0.1675	R_1 = 0.0589, wR_2 = 0.1672	R_1 = 0.0716, wR_2 = 0.1878
R indices (all data)	R_1 = 0.1453, wR_2 = 0.2605	R_1 = 0.1246, wR_2 = 0.2030	R_1 = 0.0661, wR_2 = 0.1732	R_1 = 0.0843, wR_2 = 0.1959
Absolute structure parameter	−0.10(4)	−0.014(16)	0.012(13)	0.04(2)
Largest diff. peak/hole [e·$Å^{-3}$]	0.017/−0.015	0.104/−0.110	1.382/−1.073	1.081/−0.536

gand bends away [the NB3−Co−S angle is 167.05(9)°]. The coordinated $S_2O_3^{2-}$ ion is hydrogen-bonded to the amide group of the *a* side chain (through one of the O atoms) and to the amide group of the *c* side chain (through the donor S atom). Selected bond lengths and bond angles involving the metal ion are summarised in Table 2. The Na^+ counterion is in close contact with the R8 hydroxy group and a cluster of four solvent water molecules.

The *a* side chain amide group is hydrogen-bonded to a solvent water molecule in addition to the coordinated $S_2O_3^{2-}$ ion as described above. The *b* side chain is hydrogen-bonded to the phosphate group of a neighbouring molecule. The *d* and *e* side chains are hydrogen-bonded to the *a* side chains of two different neighbours, whilst the *g* side chain hydrogen-bonds to the *e* and *b* side chains of two different neighbours. The R7 hydroxy group is involved in an intramolecular hydrogen bond to the phosphate group.

In addition to these hydrogen bonds, the cobalamin molecules are also connected to each other through the Na^+ counterion [Na−O3: 2.327(4) Å; Na−O14 (1/2 − x, −y, 1/2 + z): 2.367(4) Å]. This reinforces the interactions between molecules related by the twofold screw axis parallel to *c* as shown in Figure 7.

Solid-State Packing

The majority of cobalamins crystallise in the $P2_12_12_1$ space group.[20,29] Kratky and co-workers have shown that most of the crystal structures of cobalamins belonging to this space group can be assigned to one of four packing types. Types I−III are classified according to the *c*/*a* and *b*/*a* cell axis ratios. More recently, Randaccio et al.[29] discovered a fourth packing type, IV. The four packing types differ in the way the cobalamin molecules stack in the solid state. From the *c*/*a* and *b*/*a* cell axis ratios we have found that all four structures reported here belong to packing type I.

The Corrin Fold

The corrin fold angle (the angle between the mean planes through N21−C4−C5−C6−N22−C9−C10 and C10−C11−N23-C14−C15−C16-N24[32]) in SCNCbl is

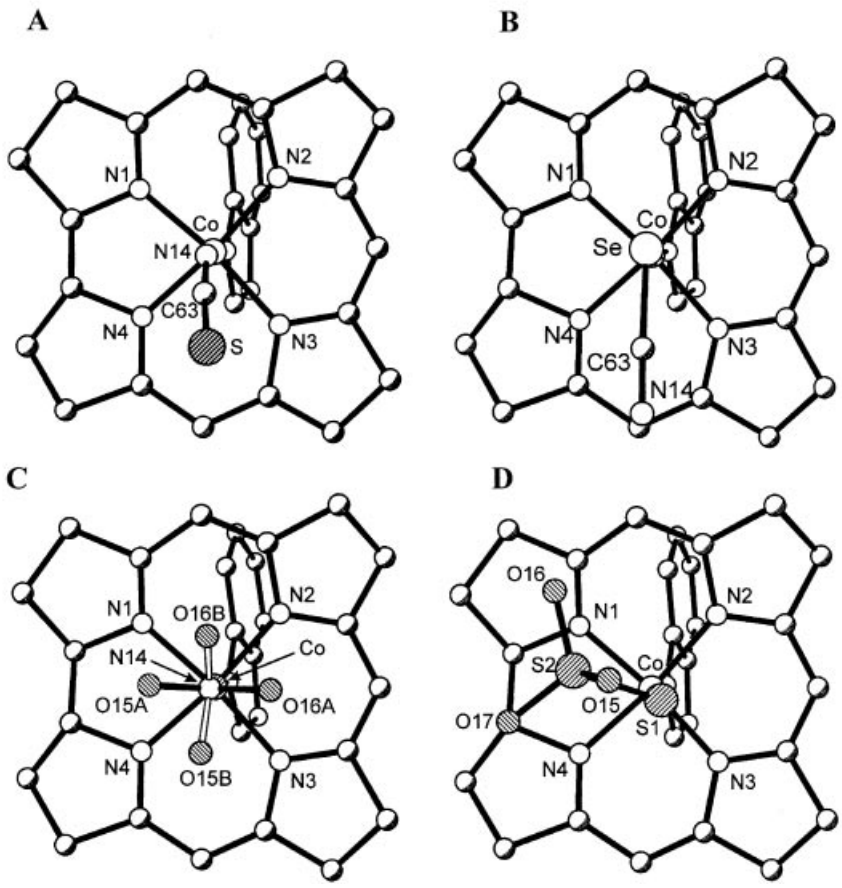

Figure 6. View of the upper face of the four corrins showing the orientation of the axial liagnds; for clarity, only the β-ligand, the corrin core, and the bzm ligand are shown

large (22.4°); of the cobalt corrinoid structures reported to date only cyano-13-*epi*-cobalamin[33] has a larger fold angle (23.7°). The fold angle in SeCNCbl is much smaller (13.7°), close to the average corrin fold angle of about 14°.[26] The fold angle is 14.5° in NO_2Cbl and somewhat larger (17.2°) in $S_2O_3Cbl^-$.

Coordinated bzm

In all the structures studied, the bzm ligand is coordinated off-vertical to the corrin ring, with a tilt angle (the angle between the mean plane through the 9 heavy atoms of the aromatic core of the bzm ligand, and the normal to the mean plane through the 24 heavy atoms of the corrin core) of 15° in SeCNCbl, 8° in NO_2Cbl, 13° in SCNCbl and 10° in $S_2O_3Cbl^-$. In each case the tilt is towards the eastern quadrant of the molecule and probably reflects the steric strain inherent in the nucleotide loop which attaches the bzm ligand to the *f* side chain through a ribose and an aminopropanol moiety (Figure 1).

Discussion

cis and *trans* Influences in Cobalamin Chemistry

The Co−NB3 bond is quite short in SCNCbl [1.958(9) Å], somewhat longer in NO_2Cbl [2.008(4) Å], and significantly longer in $S_2O_3Cbl^-$ [2.078(3) Å], SeCNCbl [2.102(7) Å] and[29,32] SO_3Cbl^- [2.134(4) Å or 2.156(5) Å] (Table 2). An examination of the Co−NB3 bond lengths in eleven cobalamins RCbl where the β-ligand is an alkyl group [adenylpropyl,[34] CF_3,[35] CH_3,[36] (*R*)- and (*S*)-2,3-dihydroxypropyl,[37] adenosyl (four separate determinations),[21,38] 2′,5′-dideoxy-5′-adenosyl and 2′,3′,5′-trideoxy-5′-adenosyl[39]] shows that the average Co−NB3 bond (2.23 ± 0.05 Å) is significantly longer than the average for the three structures XCbl (1.97 ± 0.04 Å) where the β-ligand is an inorganic moiety (X = Cl^-, N_3^- and[40] H_2O[41]). With cyanide as the *trans* ligand, the Co−NB3 bond is longer than in the XCbl systems, but shorter than in the RCbl systems (2.008 Å in CNCbl[42] and 2.023 Å in CNCbl-*b*-carboxylate[43]). There is clearly a ground-state *trans* influence; a soft or polarisable ligand in the β-position (alkyl, S- or

Table 2. Bond lengths and bond angles of the coordination sphere of Co^{III} in cobalamin complexes with ambidentate nucleophiles

Co−X−Y	SCNCbl X = N; Y = C	SeCNCbl X = Se; Y = C	NO_2Cbl X = N; Y = O	$S_2O_3Cbl^-$ X = S; Y = O	SO_3Cbl^- [a] X = S; Y = O
Co−N21	1.890(9)	1.892(6)	1.888(4)	1.881(3)	1.870(3) 1.883(5)
Co−N22	1.916(8)	1.921(7)	1.917(4)	1.915(3)	1.913(2) 1.901(5)
Co−N23	1.909(9)	1.928(7)	1.922(4)	1.915(3)	1.890(3) 1.904(5)
Co−N24	1.872(8)	1.909(6)	1.906(4)	1.893(3)	1.886(4) 1.901(5)
Co−NB3	1.955(9)	2.100(7)	2.008(4)	2.078(3)	2.134(4) 2.156(5)
Co−X	1.955(11)	2.394(2)	1.941(5)	2.2861(11)	2.231(1) 2.241(2)
N21−Co−N22	91.0(4)	89.9(3)	90.30(18)	90.33(13)	
N24−Co−N23	89.9(4)	89.6(3)	90.23(18)	90.54(13)	
N21−Co−N23	172.4(4)	173.0(3)	173.18(18)	172.83(13)	
N22−Co−N24	172.6(4)	172.7(3)	173.06(18)	172.77(13)	
N21−Co−N24	82.6(4)	83.8(3)	83.09(17)	82.92(13)	
N22−Co−N23	96.6(4)	96.9(3)	96.43(19)	96.32(13)	
N24−Co−NB3	94.5(3)	96.3(3)	95.46(18)	95.43(12)	
N21−Co−NB3	91.9(4)	91.5(3)	90.84(17)	90.80(12)	
N22−Co−NB3	89.2(4)	87.6(3)	86.69(17)	87.24(12)	
N23−Co−NB3	87.4(4)	87.1(3)	88.47(18)	86.87(12)	
N24−Co−X	87.6(4)	91.3(2)	90.31(18)	91.94(9)	
N21−Co−X	92.1(4)	90.6(2)	92.13(18)	100.67(9)	
N22−Co−X	89.1(3)	85.0(2)	87.85(18)	86.73(9)	
N23−Co−X	88.9(4)	91.6(2)	89.22(19)	82.43(9)	
NB3−Co−X	175.4(4)	172.3(2)	173.79(18)	167.07(9)	
Co−X−Y	145.7(11)	104.1(3)	121.2(4); 117.1(4) (A),[b] 129.1(11); 119.5(10) (B)[b]	122.33(6)	

[a] For comparison from Randaccio et al.[29] The reported values are for $[(SO_3)Cbl](NH_4)$. There is a more recent determination of the structure of $[(SO_3)Cbl](NH_4)$·glycerol using synchotron radiation,[63] and the results from that determination are given in italics. [b] Two positions of the NO_2 ligand.

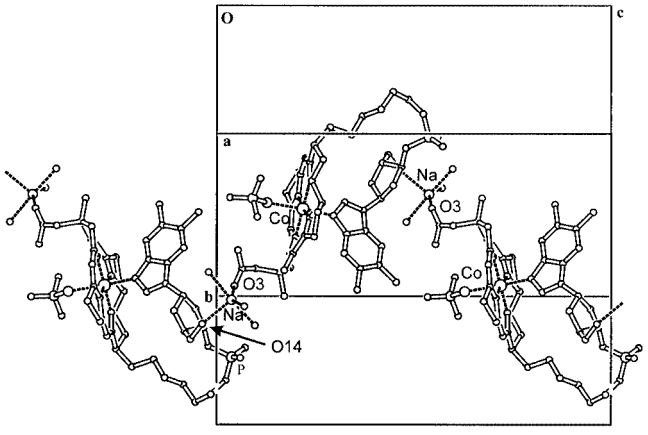

Figure 7. There is an interaction between the Na^+ counterion and oxygen atoms on neighbouring cobalamin molecules related by the twofold screw axis parallel to the *c* axis in the $S_2O_3Cbl^-$ structure; portions of the cobalamin molecules have been omitted for clarity

Se-donor as in $S_2O_3Cbl^-$ and SeCNCbl, respectively) causes an elongation of the Co−NB3 bond. The thiocyanato ligand, coordinated through N acts as a typical hard inorganic moiety, whilst coordinated NO_2^- has a similar ground-state *trans* structural influence as CN^-.

The large corrin fold angle of 22.4° in SCNCbl (the average fold angle of cobalamins in about 14°) is probably a consequence of the short Co−NB3 bond. Kratky and co-workers[20] have shown that as the axial Co−NB3 bond length decreases, the corrin fold angle increases. This is because the bzm ligand, and the B4 proton in particular, interact with the corrin ring and the corrin folds upwards towards the β-ligand in response. The corrin angles of SeCNCbl, NO_2Cbl and $S_2O_3Cbl^-$ are significantly smaller (see above).

The complexity of the UV/Vis spectra of the cobalamins makes it difficult to unambiguously determine the band positions. A plot of the apparent position of the γ-band maximum (a measure of the *cis* influence[30]) against the Co−NB3 bond length (a measure of the *trans* influence,[20] see above) shows the two parameters are correlated, albeit poorly ($r^2 = 0.58$, $n = 6$) (Figure 8, A), and the band moves to longer wavelength as the softness of the axial ligand increases. The spectrum of SCNCbl is excluded, because SCNCbl exists in solution as a mixture of the two linkage isomers, see below.

The origin of the transitions in the electronic spectrum of the corrinoids has been reviewed.[44] Kuhn and co-workers[45] used a one-dimensional free-electron model of the

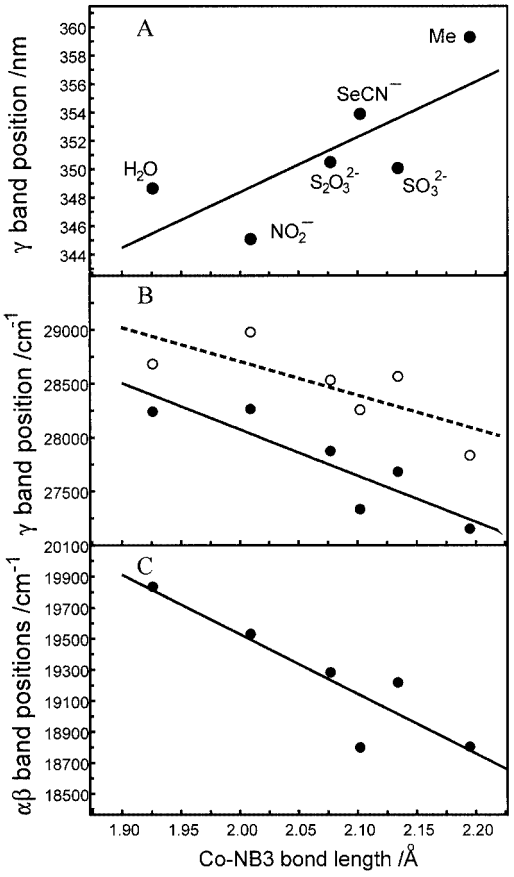

Figure 8. (A) Dependence of the apparent position of the γ-band (see Figure 3) on the Co−NB3 bond length; (B) relationship between the mean position of the three Gaussian components of the γ-band (open circles) and the two lowest-energy Gaussian components of the γ-band (filled circles) and the Co−NB3 bond length: (C) relationship between the mean position of the three components of the αβ-absorption envelope (see Figure 3) and the Co−NB3 bond length

open chain analogue of the 13-atom corrin chromophore (1,5,9,13-tetraazatrideca-1,3,5,7,9,11-pentaene) coordinated to Co^{III} to model the corrin and assign the principal bands in the electronic spectrum. In this model, the 7 lowest-energy levels of the π-electron system are occupied, and the γ-band is a symmetry-allowed transition between two states mixed by configurational interactions, $\pi_6 \rightarrow \pi_8$ and $\pi_7 \rightarrow \pi_9$. As has been noted,[46] the γ-band may be split into at least two components. The αβ-bands were assigned to the forbidden $\pi_7 \rightarrow \pi_8$ transition (the lower energy α-band) and its vibrational fine structure (the β-band). The interaction of this system with the axial ligands has been studied using an iterative extended Hückel molecular orbital method,[47] and it was shown that the main effect of the axial ligands is to change the energy of the π_7 orbital. Hence, transitions involving π_7 should shift to longer wavelength as the strength of the axial ligand field increases. Unlike the models used, the corrinoids are asymmetric with respect to rotation in the plane of the macrocycle. Since this asymmetry is expected to split these transitions, this may be the reason why both the γ- and the α,β-regions are modelled best by three Gaussian functions (Figure 4).

The three components of the γ-band were plotted against the length of the *trans*-Co−NB3 bond. Whilst the two lower energy components move to lower energy as the Co−NB3 bond length increased, there was no obvious correlation with the position of the highest-energy component, which suggests (but does not prove) that this component may not involve transitions from the π_7-molecular orbital of the corrin and may indeed not be part of the transitions that make up the γ-band. A plot of the mean position of the three Gaussian functions, and of the mean position of the two lowest-energy Gaussian functions, against the Co−NB3 bond length is shown in Figure 8, B. The latter gives a better correlation ($r^2 = 0.79$) than the former ($r^2 = 0.58$). In either case, the mean position of the components of the γ-band move to lower energy as the polarisability of the β ligand increases and the *trans*-Co−NB3 bond length increases. Similarly, all three components of the αβ-absorption envelope move to longer wavelengths as the Co−NB3 bond length increases, Figure 8, C ($r^2 = 0.81$).

This analysis indicates that there is no fundamental difference, apart from more transitions in the shorter wavelength region becoming observable, between the "typical" spectra of H_2OCbl^+, NO_2Cbl and SCNCbl, and the "atypical" spectra of $S_2O_3Cbl^-$, SeCNCbl, SO_3Cbl^- and MeCbl. The apparent differences in the γ-region stem from the components that constitute the γ-band moving apart in response to an increase in donation of electron density from the axial ligand field.

The results presented in Figure 8 are evidence for a correlation (albeit weak) between the ground-state *cis* and *trans* influences in the cobalamins. As the polarisability of the β-ligand increases, the *trans*-Co−NB3 bond length increases (*trans* influence), a consequence of the increasing electron density on the metal atom. This is transferred into the delocalised π-electron system of the corrin ring and the mean positions of the γ- and the αβ-transitions move to longer wavelength. The *trans* influence effect noted here is a further demonstration of the occurrence of a regular *trans* influence in the cobalamins as recently demonstrated by Randaccio and co-workers[32] who used DFT calculations to show that shortening of the Co−S bond in cobalamins with S-donor β-ligands causes the *trans*-Co−NB3 bond to lengthen.

The Corrin Fold

As noted above, the corrin ring in SCNCbl is considerably more folded than in SeCNCbl, NO_2Cbl or $S_2O_3Cbl^-$ (the fold angles are 22.4°, 13.7°, 14.5° and 17.2°, respectively). Examination of an overlay of the structures of SCNCbl and SeCNCbl shows that the principal reason for this is the Co−X−C−Y bond angle. When X = Se and Y = N, the small angle (104.3°) brings the axial ligand snugly between, and in close van der Waals contact with, C46 and C54 and very near the C15−C53 moiety. This forces the southern quadrant to be considerably flatter than when NCS^- is coordinated. In that case, the Co−X−C−Y (X = N, Y = S) angle is considerably larger (146.2°), and the bent axial group stands proud of C46, C54 and

C15−C53. The mean Co−N−O angle in NO_2Cbl is 121.7° and the oxygen atoms of the ligand are not in van der Waals contact with the corrin or its substituents, with the exception of the hydrogen bond formed with the *c* side chain amide group. In S_2O_3Cbl$^-$ the coordinated ligand lies along the C10···C1/C19 fold axis. Despite this, the corrin is quite folded, since the Co−S−S angle is large due to the van der Waals contacts of the ligand with the substituents in the western portion of the molecule as noted above.

The Nature of the Co^{III} Ion in Cobalamins

We have found that SCN^- coordinates to Co^{III} in SCNCbl through N. Cobalt complexes with *N*-bound thiocyanate ions are common. A survey of the Cambridge Structural Database (CSD)[48] shows that there are 37 structures containing *N*-bound SCN^- to Co^{III} with a mean Co−N bond length of 1.93 ± 0.05 Å, but only three structures with *S*-bound SCN^- (d_{Co-S} = 2.29 ± 0.03 Å). In the case of Co^{II}, 86 structures have *N*-bound NCS^-, d_{Co-N} = 2.01 ± 0.07 Å, and there is only one structure [a low-spin dicobalt(II) compound of a Schiff-base marcrocycle with four bound thiocyanato ligands, two *N*-bound and two *S*-bound[49]] with *S*-bound SCN^- (d_{Co-S} = 2.584 Å). Hence, irrespective of the oxidation state of the metal ion, there is a strong preference for the thiocyanate ion to coordinate through N.

As expected, NO_2^- forms a longer bond to low-spin d^7 Co^{II} than it does to low-spin d^6 Co^{III}. The Co−NCS bond of 1.954(11) Å in SCNCbl is marginally long for coordination to Co^{III} (mean 1.93 ± 0.05 Å, see above), but short for coordination to Co^{II} (mean 2.01 ± 0.07 Å). It could be argued that the crowded β-face of the corrin ring contributes to Co−N bond lengthening. However, the Co−N−C angle is 146.2(11)°, which is close to the smallest angle (140.7°) found in the CSD for *N*-bound SCN^- to Co^{III} (the range is 140.7−178.8°, with an average value of 168 ± 8°). The analogous data for Co^{II} are 137.4−179.5°, 166 ± 8°. One would expect the angle to be considerably larger if there was a significant steric effect. The slightly long Co−N bond to NCS^- in SCNCbl is not due to steric reasons and could be the result of some partial Co^{II} character of the metal ion.

There is a report[50] of a crystal structure of SCNCbl in which the thiocyanato ligand is bound through S. The ^{1}H and ^{13}C NMR data of a solution containing B_{12a} and sufficient SCN^- for complete complex formation (the formation constant of the thiocyanato complex is log *K* = 3.1[51]) at 25 °C contains two sets of peaks close to each other, indicative of two different but related species in solution, which we assumed to be the linkage isomers. The peaks in the ^{1}H NMR spectrum due to the C10 and C13 protons are relatively free of overlap and were integrated, giving ratios of 1:0.75 and 1:0.86, respectively. (We have not been able to assign the individual resonances to each of the two linkage isomers.) SCNCbl clearly exists in solution as a mixture of the *N*- and the *S*-bound isomers and it is perhaps fortuitous that we obtained the *N*-bound isomer.

Addition of excess KSeCN to a solution of B_{12a} results in the immediate formation of a purple solution which, over time, changes to a solution with a more distinctly red colour. The initial ^{1}H and ^{13}C NMR spectra are consistent with a single product, and there is an apparently smooth transition to a second product with a half-life of about 2 d. The UV/Vis and ^{13}C NMR spectra of the final product are identical to those of CNCbl. Analysis of the X-ray diffraction of crystals obtained from the aged solution confirmed that the product is CNCbl (data not reported). This process occurs both under aerobic and anaerobic conditions. Since the crystal structure of the initial compound shows the ligand to be *Se*-bound, and there is no evidence for linkage isomerism in the ^{1}H and ^{13}C NMR spectra, we conclude that the selenocyanato complex decomposes slowly with extrusion of Se to form CNCbl. To date we have made no attempt to explore the mechanism of this reaction, but we note a report that [Ru(bmipy)(dcbpy)I]$^-$ [dcbpy^{2-} = 4,4′-dicarboxy-2,2′-bipyridyl; bmipy = 2,6-bis(1-methylbenzimidazol-2-yl)pyridyl] reacts with $SeCN^-$ to form a mixture of the *Se*- and the *N*-bound complexes. Prolonged reaction produces only the *N*-bound isomer which then rapidly yields the cyano complex with extrusion of Se.[52] Also, when *cis*-L_2Ru$(NCS)_2$ (L_2 = diethyl 2,2′-bipyridyl-4,4′-dicarboxylate) is oxidised to Ru^{III}, S is eliminated and the dicyanato complex is produced.[53] These workers noted that the reaction mechanism is complex, and postulated that extrusion of S occurs through a cyclic intermediate and rearrangement from *N*- to *C*-bound cyanide ion. Since $SeCN^-$ is coordinated to cobalamin in a bent fashion, an analogous cyclic intermediate appears to be feasible in the Se extrusion pathway.

There is only one example of a Co^{III}−selenocyanate complex in the CSD (a diselenocyanato cobaloxime complex[54]) and no complexes of Co^{II}. The Co^{III} compound has the ligand *Se*-bound to the metal atom with a Co−Se bond length of 2.383 Å, a Co−Se−C angle of 106.2° and an Se−N−C angle of 175.5°. Hence, the geometry is quite similar to that of SeCNCbl where the analogous parameters are 2.394 Å, 104.3° and 176.2°. Thus, the cobalt ions in the cobalamins behave like Co^{III} towards $SeCN^-$.

The great majority of NO_2^- complexes of Co^{III} reported in the CSD (148 structures) have the ligand bonded through the softer N donor with a mean Co−N bond length of 1.94(3) Å, an N−O bond length of 1.22(3) Å, a Co−N−O bond angle of between 112° and 132° [mean 120(2)°] and an O−N−O angle of between 92° and 135° [mean 119(3)°]. There are only two structures with *O*-bound NO_2^- [the mean Co−O bond length is 1.90(4) Å]. The two available structures of NO_2^- complexes of Co^{II} both have the ligand bonded through N. The Co−N bond lengths vary between 1.889 and 1.944 Å [mean 1.92(6) Å]. Surprisingly, the average Co^{II}−N bond is somewhat shorter than the average Co^{III}−N bond and this may be indicative of some metal-to-ligand back-bonding. The NO_2Cbl structure is therefore typical for coordination of NO_2^- to Co^{III} [the results for the major occupied site has Co−N = 1.941(5) Å, N−O = 1.230(2) Å, Co−N−O = 121.1(4)° and 117.2(4)° and

O−N−O = 121.6(5)°]. The ^1H and ^{13}C NMR spectra indicate the presence of a single compound in solution and the kinetic data (see Introduction) are consistent with reaction through N. There is therefore no evidence for the nitrito isomer.

Although there are relatively few structures of complexes containing $S_2O_3^{2-}$ coordinated to cobalt (there is one with Co^{II}, and six with Co^{III}), those which have been reported are all *S*-bonded. There are significant differences in the lengths of the Co−S bonds: 2.488 Å in the *cis*-bis(thiosulfato)tetraaquacobalt(II) ion[55] and, on average, 2.28(3) Å in the Co^{III} complexes. In the latter, the average Co−S−S bond angle is 112(2)°. Therefore, the observed bond length of 2.286(1) Å in $S_2O_3Cbl^-$ is consistent with coordination to a Co^{III} centre. The somewhat large Co−S−S bond angle of 122.35(6)° is probably a consequence of close steric contact with the *a* side chain.

Conclusion

The lability of the formally low-spin Co^{III} centre in cobalamins, a notable feature of B_{12} chemistry (see Figure 2), is clearly conferred by the equatorial corrin ligand. There is clear evidence of electronic communication between the equatorial ligand system and the axial coordination sites of the metal ion. Thus, the principal transitions in the electronic spectra of the cobalamins shift to longer wavelengths as the donor power of the β-ligand increases (Figures 3 and 8). In addition to this *cis* influence, there is a normal *trans* influence as the Co−NB3 bond length responds to the donor ability of the β-ligand (Figure 8).

The structures of four cobalamin complexes obtained by the displacement of the axial H_2O molecule of B_{12a} with ambident nucleophiles (SCN^-, $SeCN^-$, NO_2^- and $S_2O_3^{2-}$) have been determined by X-ray diffraction methods. Our results show that Co^{III} in the complexes studied usually binds to the softer of the two available donor atoms (Se rather than N in $SeCN^-$, N rather than O in NO_2^- and S rather than O in $S_2O_3^{2-}$), but SCN^- is found to be *N*-bound in the solid state. However, there is a previous report of an *S*-bound complex and SCNCbl exists as a mixture of the two linkage isomers in solution. This preference for the softer donor atom in ambidentate nucleophiles is not unusual for cobalt complexes. An examination of the structures available in the CSD shows that irrespective of the oxidation state of the Co centre (+2 or +3), there is a strong preference for the thiocyanate ion to coordinate to the cobalt atom through N. The only example of a Co^{III}−selenocyanato complex in the CSD has the ligand bound through Se. NO_2^- usually coordinates to Co^{III} through N. The two Co^{II} structures available with NO_2^- as a ligand also have the ligand *N*-bound. There are relatively few structures of $S_2O_3^{2-}$ coordinated to Co^{II} and Co^{III}; all are *S*-bound.

If the metal ion in the cobalamins had significant Co^{II}-like character, then the bond to the β-axial ligand should be long, consistent with population of d_{z^2} in a pseudo-octahedral ligand field; in Co^{II} corrinoids the β-ligand is either absent or, at most, interacts very weakly with the metal centre. The Co−N bond in SCNCbl is marginally long for coordination to Co^{III} [$d_{Co^{III}-N}$ = 1.93 ± 0.05 Å; 1.954(11) Å observed in SCNCbl]. However, the other complexes have bond lengths expected for coordination to Co^{III}. Therefore, the increase in electron density that the corrin undoubtedly imparts to the metal atom has no significant effect on the ground-state structures of these complexes.

Experimental Section

UV/Vis Studies: UV/Vis spectra were recorded using a Cary 3E spectrophotometer with the cell compartment thermostatted by a water-circulating bath. These spectra, as well as those of SO_3Cbl^- and CH_3Cbl, the crystal structures of which have been reported by others, were analysed by Gaussian analysis, as we have done previously for iron porphyrins.[56] Each spectrum was converted into a plot of absorbance against wavenumber and fitted to the sum of the minimum number of Gaussian bands [Equation (2)] using non-linear least squares.[57] In Equation (2), A_T is the total absorbance, λ the measured wavenumber, λ_j the wavenumber at which the *j*th Gaussian component reaches a maximum absorbance, α_j the intensity of the *j*th peak and Δ_j the half-width of the *j*th band at 0.607 of the maximum intensity.

$$A_T = \sum_{j=1}^{n} \alpha_j \exp\left[\frac{-(\lambda - \lambda_j)^2}{2\Delta_j^2}\right] \quad (2)$$

Single Crystal X-ray Structure Determinations: Crystals were grown by dissolving hydroxocobalamin (approximately 50 mg, Roussel, > 99% pure, HPLC) in deionised water (700 μL) . To this was added an excess of the salt of the ligand. The solution was gently heated to ensure dissolution. The crystals were grown in H-tubes in a refrigerator, by vapour diffusion of acetone into the aqueous solution. Crystals usually appeared after about a week. A suitable crystal was selected after visual examination under a microscope. Intensity data were collected with a Bruker SMART 1 K CCD area detector diffractometer with graphite-monochromated Mo-K_α radiation (50 kV, 30 mA). The collection method involved ω-scans of 0.3° width. Data reduction was carried out using the program SAINT+[58] and absorption corrections were made using the program SADABS.[59] The crystal structures were solved by direct methods using SHELXS-97.[60] All non-hydrogen atoms of the cobalamin were first refined isotropically followed by anisotropic refinement by full-matrix least-squares calculations based on F^2 with SHELX-97 until convergence was achieved. Hydrogen atoms were positioned geometrically and allowed to ride on their respective parent atoms. In most cases it was not possible to locate the hydrogen atoms on the water molecules. These have been included in the formula sum, however. Diagrams and publication material were generated using WinGX[61] and PLATON.[62] CCDC-185962 to -185965 contain the supplementary crystallographic data for this paper. These data can be obtained free of charge at www.ccdc.cam.ac.uk/conts/retrieving.html [or from the Cambridge Crystallographic Data Centre, 12 Union Road, Cambridge CB2 1EZ, UK; Fax: (internat.) + 44-1223/336-033; E-mail: deposit@ccdc.cam.ac.uk].

X-ray Structure Determination of SCNCbl: SCNCbl was found to contain some disordered guest water molecules. These were mod-

elled over two positions by either fixing their occupancies, or by assigning their occupancies to a free variable and allowing the free variable to be refined.

X-ray Structure Determination of SeCNCbl: All the solvent molecules in SeCNCbl were refined anisotropically with full occupancies.

X-ray Structure Determination of NO_2Cbl: Disordered atoms in the main body of the NO_2Cbl structure were refined independently with individual isotropic temperature factors. Disordered moieties included the NO_2 ligand and the *c* and *e* side chains. The NO_2 ligand was modelled over two orientations, with a site occupancy ratio of 0.82:0.18. The *c* and *e* side chains were both modelled over two orientations in 0.63:0.37 and 0.61:0.39 site occupancy ratios, respectively. Soft SADI restraints were used to ensure that all the bond lengths between the same atoms in each orientation were similar. The unit cell of NO_2Cbl contained a solvent acetone molecule in addition to several water solvent molecules. All C−C bonds, and the C−O bond in the acetone molecule were restrained to 1.50(2) and 1.24(2) Å, respectively, and a FLAT restraint was used to ensure that all the atoms were planar. Many of the water molecules in the NO_2Cbl structure were found to be disordered, or partially present. These were refined independently with individual isotropic thermal factors if the refinement was unstable.

X-ray Structure Determination of NaS_2O_3Cbl: The acetone solvent molecule in the $S_2O_3Cbl^-$ structure was refined isotropically, and all C−C and C−O bonds were restrained to 1.50(2) and 1.24(2) Å, respectively. All atoms in the acetone molecule were kept in a plane with the FLAT restraint. As with the previous structures, some of the solvent water molecules were refined and fixed with partial occupancies or, if they were disordered, modelled over two orientations. These solvent molecules were refined isotropically if anisotropic refinements resulted in unstable thermal parameters. ISOR restraints were applied to some of the solvent water molecules to approximate their U_{ij} values to isotropic behaviour.

Acknowledgments

This work was sponsored by the National Research Foundation, Pretoria, the University of the Witwatersrand through the Molecular Sciences Institute (H. M. M.) and the National Institute of Health (USA), grant GM48858 (K. L. B.).

[1] H. M. Marques, L. Knapton, *J. Chem. Soc., Dalton Trans.* **1997**, 3827−3833.
[2] J. J. P. Stewart, *J. Comput. Chem.* **1989**, *10*, 209−220.
[3] J. J. P. Stewart, *J. Comput. Chem.* **1989**, *10*, 221−264.
[4] R. G. Pearson, *J. Am. Chem. Soc.* **1963**, *85*, 3533−3539.
[5] K. L. Brown, S. Cheng, X. Zou, J. D. Zubkowski, E. J. Valente, L. Knapton, H. M. Marques, *Inorg. Chem.* **1997**, *36*, 3666−3675.
[6] C. K. Poon, *Coord. Chem. Rev.* **1973**, *10*, 1−35.
[7] A. D. Bacon, M. C. Zerner, *Theor. Chim. Acta* **1979**, *53*, 21−54.
[8] W. P. Anderson, W. D. Edwards, M. C. Zerner, *Inorg. Chem.* **1986**, *25*, 2728−2732.
[9] H. M. Marques, L. Knapton, X. Zou, K. L. Brown, *J. Chem. Soc., Dalton Trans.* **2002**, 3195−3200.
[10] H. M. Marques, L. Knapton, unpublished results.
[11] R. G. Finke, D. A. Schiraldi, B. J. Mayer, *Coord. Chem. Rev.* **1984**, *54*, 1−22.
[12] J. Halpern, *Science (Washington, DC, U. S.)* **1985**, *227*, 869−875.
[13] R. Banerjee, S. Chowdhury, in *Chemistry and Biochemistry of B_{12}* (Ed.: R. Banerjee), Wiley, New York, **1999**, pp. 707−729.
[14] R. G. Finke, B. P. Hay, *Inorg. Chem.* **1984**, *23*, 3041−3043.
[15] B. P. Hay, R. G. Finke, *J. Am. Chem. Soc.* **1986**, *108*, 4820−4829.
[16] K. L. Brown, S. Cheng, J. D. Zubkowski, E. J. Valente, *Inorg. Chem.* **1997**, *36*, 1772−1781.
[17] B. D. Martin, R. G. Finke, *J. Am. Chem. Soc.* **1992**, *114*, 585−592.
[18] B. Kräutler, W. Keller, M. Hughes, C. Caderas, C. Kratky, *J. Chem. Soc., Chem. Commun.* **1987**, 1678−1680.
[19] B. Kräutler, W. Keller, C. Kratky, *J. Am. Chem. Soc.* **1989**, *111*, 8936−8938.
[20] K. Gruber, G. Jogl, G. Klintschar, C. Kratky, in *Vitamin B_{12} and B_{12} Proteins* (Eds.: B. Kräutler, D. Arigoni, B. T. Golding), Wiley-VCH, New York, **1998**, pp. 335−347.
[21] P. G. Lenhert, *Proc. Royal Soc., London* **1968**, *A303*, 45−84.
[22] B. Kräutler, R. Konrat, E. Stupperich, G. Färber, K. Gruber, C. Kratky, *Inorg. Chem.* **1994**, *33*, 4128−4136.
[23] C. L. Drennan, S. Huang, J. T. Drummond, R. G. Matthews, M. L. Ludwig, *Science (Washington, DC, U. S.)* **1994**, *226*, 1669−1674.
[24] F. Mancia, N. H. Keep, A. Nakagawa, P. F. Leadlay, S. McSweeny, B. Rasmussen, P. Bosecke, O. Diat, P. R. Evans, *Structure* **1996**, *4*, 339−350.
[25] M. L. Ludwig, P. R. Evans, in *Chemistry and Biochemistry of B_{12}* (Ed.: R. Banerjee), Wiley, New York, **1999**, pp. 595−632.
[26] C. Kratky, B. Kräutler, in *Chemistry and Biochemistry of B_{12}* (Ed.:R. Banerjee), Wiley, New York, **1999**, pp. 9−41.
[27] J. M. Pratt, in *Chemistry and Biochemistry of B_{12}* (Ed.: R. Banerjee), Wiley, New York, **1999**, pp. 73−112.
[28] R. T. Taylor, in *B_{12}* (Ed.: D. Dolphin), Wiley, New York, **1982**, vol. 2, pp. 307−355.
[29] L. Randaccio, S. Geremia, G. Nardin, M. Slouf, I. Srnova, *Inorg. Chem.* **1999**, *38*, 4087−4092.
[30] J. M. Pratt, in *Chemistry and Biochemistry of B_{12}* (Ed.: R. Banerjee), Wiley, New York, **1999**, pp. 113−164.
[31] M. Nardelli, *J. Appl. Crystallogr.* **1995**, *28*, 659−659.
[32] J. P. Glusker in *B_{12}* (Ed.:D. Dolphin), Wiley, New York, **1982**, vol. 1, pp. 23−106.
[33] K. L. Brown, D. R. Evans, J. D. Zubkowski, E. J. Valente, *Inorg. Chem.* **1996**, *35*, 415−423.
[34] T. G. Pagano, L. G. Marzilli, M. M. Flocco, C. Tsai, H. L. Carrell, J. P. Glusker, *J. Am. Chem. Soc.* **1991**, *113*, 531−542.
[35] K. L. Brown, X. Zou, *Inorg. Chim. Acta* **1998**, *267*, 305−308.
[36] M. Rossi, J. P. Glusker, L. Randaccio, L. G. Marzilli, *J. Am. Chem. Soc.* **1985**, *107*, 1729−1738.
[37] N. W. Alcock, R. M. Dixon, B. T. Goulding, *J. Chem. Soc., Chem. Commun.* **1985**, 603−605.
[38] F. J. Savage, P. F. Lindley, J. L. Finney, P. A. Timmins, *Acta Crystallogr., Sect. B* **1987**, *43*, 280−295.
[39] B. Kräutler, in: "Organic Reactivity: Physical and Biological Aspects" (Eds.: B. T. Golding, R. J. Griffin, H. Maskill), *Spec. Publ. - R. Soc. Chem.* **1995**, 148, 209−214. Coordinates supplied by: C. Kratky, Karl-Franzens-Universität, Graz, Austria.
[40] L. Randaccio, S. Geremia, M. Furlan, M. Slouf, *Inorg. Chem.* **1998**, *37*, 5390−5393.
[41] C. Kratky, G. Fäber, K. Gruber, K. Wilson, Z. Dauter, H.-F. Nolting, R. Konrat, B. Kräutler, *J. Am. Chem. Soc.* **1995**, *117*, 4654−4670.
[42] B. Kräutler, R. Konrat, E. Stupperich, G. Fäber, K. Gruber, C. Kratky, *Inorg. Chem.* **1994**, *33*, 4128−4139.
[43] J. M. Waters, T. N. M. Waters, *Proc. Indian Acad. Sci.* **1984**, *93*, 219−234.
[44] C. Giannotti, in *B_{12}* (Ed.: D. Dolphin), Academic Press, New York, **1982**, pp. 393−430.
[45] H. Kuhn, K. H. Drexhage, H. Martin, *Proc. R. Soc.* **1965**, *288*, 348−351.

[46] P. O. Offenhartz, B. H. Offenhartz, M. M. Fung, *J. Am. Chem. Soc.* **1970**, *92*, 2966−2973.
[47] G. N. Schrauzer, *Naturwissenschaften* **1966**, *53*, 459−463.
[48] Version 5.22, Oct. 2001 release: F. H. Allen, *Acta Crystallogr., Sect. B* **2002**, *58*, 380−388.
[49] S. Brooker, P. G. Plieger, B. Moubaraki, K. S. Murray, *Angew. Chem. Int. Ed.* **1999**, *38*, 408−410.
[50] Personal communication with D. C. Hodgkin, quoted by J. M. Pratt, *Inorganic Chemistry of B_{12}*, Academic Press, London, **1972**, p. 152.
[51] J. M. Pratt, *Inorganic Chemistry of B_{12}*, Academic Press, London, **1972**, p. 58.
[52] O. Kohle, S. Ruile, M. Grätzel, *Inorg. Chem.* **1996**, *35*, 4779−4787.
[53] G. Wolfbauer, A. M. Bond, D. R. MacFarlane, *Inorg. Chem.* **1999**, *38*, 3836−3846.
[54] I. D. Samus, N. V. Belov, *Dokl. Akad. Nauk SSSR* **1970**, *193*, 333−336.
[55] A. Carter, M. G. B. Drew, *Polyhedron* **1999**, *18*, 1445−1453.
[56] O. Q. Munro, H. M. Marques, *Inorg. Chem.* **1996**, *35*, 3768−3779.
[57] G. Brink, *FIT, a computer program for non-linear least-squares fitting using the Marquard algorithm*, University of the Witwatersrand, Johannesburg, South Africa, **1992**.
[58] *SAINT+*, Version 6.02 (includes XPREP and SADABS), Bruker AXS Inc., Madison, Wisconsin, USA, **1999**.
[59] G. M. Sheldrick, *SADABS*, University of Göttingen, Germany, **1996**.
[60] G. M. Sheldrick, *SHELXS-97*, release 97-2, University of Göttingen, Germany, **1997**.
[61] WinGX, Version 1.63.01: L. J. Farrugia, *J. Appl. Crystallogr.* **1999**, *32*, 837−838.
[62] A. L. Spek, *Acta Crystallogr., Sect. A* **1990**, *46*, C34−C34.
[63] L. Randaccio, S. Geremia, M. Stener, D. Toffoli, E. Zangrando, *Eur. J. Inorg. Chem.* **2002**, 93−103.

Received October 31, 2002

